

Completion of the production of the W7-X divertor target modules

J. Boscary^a, G. Ehrke^b, H. Greuner^a, P. Junghanns^a, C. Li^a,
B. Mendelevitch^a, J. Springer^a, R. Stadler^a, W7-X Team^c

^aMax-Planck-Institut für Plasmaphysik, Boltzmannstr. 2, 85748 Garching, Germany

^bMax-Planck-Institut für Plasmaphysik, Wendelsteinstr. 1, 17498 Greifswald, Germany

^cT. Klinger et al., Nucl. Fusion 59 (2019) 112004 doi: 10.1088/1741-4326/ab03a7

The installation of an actively water cooled divertor in the stellarator Wendelstein 7-X (W7X) is mandatory to achieve stationary power and particle exhaust for pulse lengths up to 30 min. The highly loaded divertor area is made of 100 target modules distributed in ten divertor units. The target modules have mechanical support frames with attachment systems to the plasma vessel, and manifolds to distribute water equally between the target elements. A target element is designed to remove a stationary heat flux up to 10 MW/m² and is made of a CuCrZr copper alloy heat sink armored with CFC NB31 tiles. The manufacturing process, assembly and quality assessment of the last 70 target modules has been successfully completed in the Integrated Technical Centre of IPP-Garching. Some parts such as the target elements and manifolds were delivered by industry. The quality was assessed as follows: visual inspections, measurement of the 3-D CFC surface, dynamic pressure tests, He leak testing under pressure at different temperature (20°C, 160°C) in vacuum oven, high heat flux testing. The production of the water cooled divertor is now completed, and the mounting operation of the target modules in the plasma vessel of W7-X has started.

Keywords: Stellarator, Wendelstein 7-X, Plasma Facing Component, Divertor.

1. Introduction

The stellarator Wendelstein 7-X (W7-X) started successfully short pulse divertor operation with un-cooled modular divertor made of fine-grained graphite tiles [1, 2]. For the upcoming steady-state operation with pulse length up to 1800 sec. and continuous plasma heating with up to 10 MW electron cyclotron resonance heating (ECRH), the installation of an actively water cooled HHF (high heat flux) divertor together with a cryo-vacuum pump system [3] is mandatory. The function of the divertor is to control the plasma power and particle exhaust. A detailed description of the other in vessel components such as baffles, divertor closures, and first wall is given in [4, 5, 6].

The W7-X divertor consists of 10 similar discrete divertor units, one positioned above and one below the helical axis in each of the five symmetric field periods. The design of the target area, which defines the convectively loaded surface of the divertor, is based on nine reference plasma configurations and, with a total surface of 25.6 m², offers a high degree of experimental flexibility [7]. The target area was originally designed to remove stationary heat fluxes up to 10 MW/m²; an intermediate lower loaded area of a total of 6 m² was introduced to reduce the highly loaded surface [8]. The target areas are shown in Fig. 1: the highly loaded vertical and horizontal target areas positioned on the inboard and outboard sides of the plasma vessel, respectively, and the high iota tail with an intermediate lower loaded surface.

The highly loaded target area consists of 890 target elements (TEs) assembled to 100 HHF Target Modules (TMs), 10 in each divertor unit: TM1H, 2H, 3H, 4H for the horizontal targets, TM1V, 2V, 3V for the vertical targets, and TM7H, 8H, 9H for the high iota tail. The

lower heat flux (LHF) loaded target area consists of 20 LHF TMs, 2 in each divertor unit, namely TM5H and 6H. This paper focuses on the production of the last 70 produced TMs of the vertical and horizontal target areas with a toroidal angle between +18° and +1,4 (Fig.1). The successive steps of the TM production are presented: preparation phase, manufacturing process and results of the quality assessment. The production of the TMs of the high iota tail (TM7H, 8H, 9H) can be found in [9].

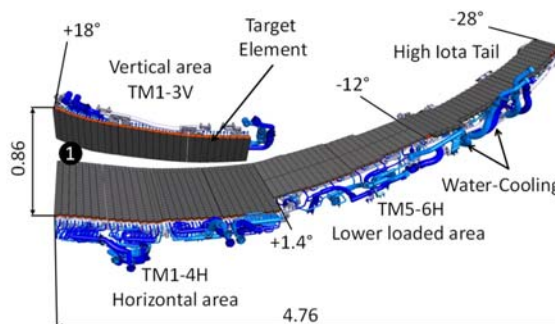


Fig. 1. Main target areas of one divertor unit. Outer dimensions are in m. The divertor is an open structure with the horizontal and vertical targets, which define the main pumping gap ①. Other divertor components such as baffles and divertor closures are not shown.

2. Target Element

The production of the TEs was awarded to the company Plansee SE, Austria in 2004. The last delivery arrived at IPP in 2014. A TE is made of a CuCrZr copper alloy heat sink armored with carbon fibre reinforced carbon CFC NB31 tiles. It is designed to remove a stationary heat flux up to 10 MW/m² on its main top surface, and 5 MW/m² on the last top tile on the side of the pumping gap. Depending on the design requirements

the water connectors of the TEs are perpendicular and parallel to the TE axis, respectively. The results of the production and quality assessment of the TEs are summarized in [10, 11]. After delivery, a minor number of TEs were repaired [12, 13]. Before installation in the TMs, the TEs were individually 3D-machined to fit uniformly the plasma-facing surface [14].

3. Target Module

The production of the TMs was organized in the Integrated Technical Centre (ITZ) of IPP-Garching in two parallel lines: one for the vertical and another one for the horizontal TMs. Different grades of stainless steel were used for the TMs: DIN 1.4429 (X2CrNiMo17-13-3) for supporting frames, DIN 1.4311 (X2CrNi18-10) for flanges, DIN 1.4125 (X105CrMo17) for bolts, DIN 1.4429 or 1.4435 (X2CrNiMo18-14-3) for brackets, DIN 1.4301 (X5CrNi18-10) for slices, DIN 1.4311 or 1.4980 (X6NiCrTiMoVB25-15-2) for sockets. Stainless steel was certified with a cobalt content ≤ 500 ppm, and a relative magnetic permeability ≤ 1.01 , except weld seams < 1.05 . Main features of the TMs are shown in Table 1. Length is in the poloidal direction, and width in the toroidal direction.

Table 1. Main dimensions of the target modules

TM type	Length (mm)	Width (mm)	Height (mm)	Weight (kg)
TM1H	799	411	173	61
TM2H	787	422	184	60
TM3H	804	455	224	70
TM4H	768	471	239	71
TM1V	555	363	160	56
TM2V	557	363	125	68
TM3V	500	363	145	47

3.1 Surface of the target modules

The surface of the TMs is made of consecutive TEs in the toroidal direction. The 3D-machined TEs were installed onto bearing frames with a max. ± 0.1 mm step between neighboring TEs before welding the water connectors to the cooling pipes. The bearing surfaces were machined with a tolerance of 0.05 mm between neighboring surfaces. The TE positions were measured with a Zeiss machine of type Accura II. The measured points were always compared to the corresponding points of the CAD-surface with a ± 0.5 mm requirement in the same coordinate system. The CuCrZr heat sinks were manufactured with studs to screw the TEs into the holes of the bearing frames via disc spring stacks with a 7 Nm torque [10]. The number of studs depends on the TE length. The TEs of the vertical area (361 mm long) have two studs. The TEs of the horizontal area (572-594 mm long) have three studs. The holes of the bearing frames on the side of the water connectors were machined for fixed points and the other ones for slotted holes to allow thermal expansion in the length direction.

Fig. 2 and Fig. 3 illustrate the difference of the divertor surface between the vertical and horizontal areas. Fig. 2 shows the positioning of the 3D machined TEs onto the bearing rails of TM1V from the back side. This figure

shows the significant curvature towards the plasma of the divertor surface at this location.

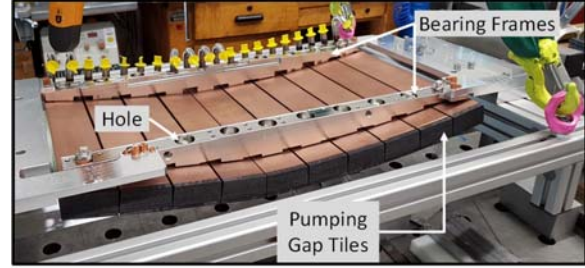


Fig. 2. Positioning of the TEs on the bearing frames to form the divertor surface before welding the water connectors to the cooling pipes. At this stage, water connectors are closed with yellow plugs and the TM is fixed to an ITEM frame for easy transport.

Fig. 3 shows TM1H and TM2H placed side by side. The resulting surface is slightly curved with a stronger curvature at the edge of TM1H.

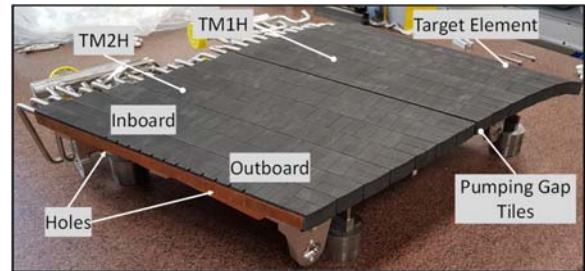


Fig. 3. Positioning of TM1H and TM2H side by side. Integration of pop-up of Langmuir probes in TM2H. The TE length is 594 mm. Slit of 0.4 mm between adjacent tiles (25 mm size in the poloidal direction) are visible.

In this area, different types of diagnostics have been integrated in the divertor surface. As example, Fig. 4 shows the 12 apertures (3×4 mm²) manufactured at the edge of TM2H to allow the integration of the pop-up array of Langmuir probes between TM2H and TM3H. At this location, wall thickness of the TE is increased to 4.5 mm on one side. The sides of the holes were, in addition, locally machined to avoid leading edge. The same kind of apertures have been machined at the edge of the neighboring TM3H.



Fig. 4: Apertures machined in TM2H for the integration of the pop-up array of Langmuir probes.

As shown in Fig. 1, the vertical and horizontal TMs define the main divertor pumping gap; the cryo-vacuum pump is positioned under TM1-4H in each divertor unit. The TEs are in addition armored with tiles on the side facing the pumping gap which are designed for up to 2 MW/m² [15]. On the vertical side, the boundary along the pumping gap is mostly straight in the toroidal direction. On the horizontal side, the situation is different with a curved boundary along the pumping gap in the toroidal direction as illustrated in the CAD view of one divertor

unit in Fig. 1. Fig. 5 shows the facets in the middle of the tiles of the TEs of TM2H facing the pumping gap, which were manufactured to avoid possible leading edges. This decision to cover these ends of the targets was taken at a very late stage after starting the production of the CFC NB31 blocks. The size of the blocks did not allow the fabrication of this kind of tiles for the non standard TEs designed for diagnostics. At this location, two small tiles have been positioned.

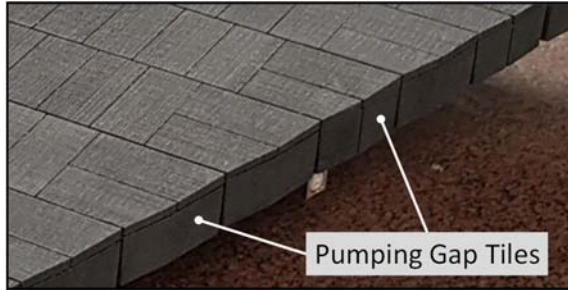


Fig. 5: CFC tiles protecting the end of the target elements of TM2H along the pumping gap.

3.2 Cooling system of the target modules

The piping system of the TMs is assembled from two sub-groups: manifolds + pipes, and TEs + pipes. The design has to take into account not only the available space but also the deformation of the TMs in operation and the final assembly sequence of the connection to the water feeding pipes of the plug-ins via CF-flanges in the plasma vessel. The design of the pipes was checked to ensure it has enough flexibility to allow thermal movements. A total of 1530 orbital welds was needed to complete the cooling system at ITZ.

The pipes are made of $\text{Ø}12 \times 1$ mm stainless steel, according to DIN 1.4429. The housing of the manifold is made of DIN 1.4429 and the branch stubs of DIN 1.4435 stainless steel. The connections between TEs, pipes and manifolds were made by TIG (Tungsten Inert Gas) orbital welding with full penetration and without filler material. The qualification of this process and the difficulties encountered during the production taking into account the thermo-capillary convection (Marangoni effect) are detailed in [9].



Fig. 6. Example of the manufacturing process of the sub-group manifold + pipes for TM1V.

Fig. 6 shows the positioning of the manifolds on the jigs made of aluminium for TM1V. The pipes were already welded to the branches of the manifolds. The pipe routing is machined in the jig and the final position (axis of the tube) of the other end to get parallel surfaces to be

welded to the water connectors of the TEs in a following step is set.

The manifolds procured from the company Dockweiler, Germany, are based on the “collaring” technology, which allows inside welding of branch stubs to avoid gaps and ensure smooth surfaces. For the TM1-4H, 40 manifolds with 8 different types of ($\text{Ø}38$ mm, 2 mm thick) with length varying from 219 to 340 mm were produced. The manifolds were delivered with CF-flanges to connect to the water supply system. Support blocks were welded on the manifolds to maintain the manifolds in position; in a following stage they were screwed onto the plates of support frames of the TMs.

Due to the restricted available space, special solutions were developed in the vertical area for the design of the manifolds. The manifolds were bent or the diameter was reduced to 26,9 mm (compared to the standard diameter of 38 mm) on 35% of its length. For TM2V, one manifold has also a reduced diameter of 26,9 mm on 60% of its length.

The standard solution for the connection of the TMs to the pipes of the plug-ins is via flexible hoses to allow for thermal expansion and for installation tolerances. This design was not possible in the vertical area. The hoses have been replaced there by lateral compensators. A compensator is made of an expansion joints constrained into a cage to define the axial pressure force. The drilled pipe is made of stainless steel according to DIN 1.4429 and the bellow to DIN 1.4404 (X2CrNiMo17-12-2). The effective spring rate within $\pm 30\%$ is 70 N/mm (axial) and 110 N/mm (lateral) at 20 and 60°C. It has been designed for the following load cases: (1) for mounting operation, 10 cycles with a maximal displacement of ± 3.5 mm axially and ± 2.5 mm laterally, (2) in operation, 30,000 cycles with ± 0.7 mm axially and ± 0.5 mm laterally. The dimensions of the bellow are: 120,7 mm long, 50 mm outer diameter, 34 mm inner diameter. In particular it provides sufficient space to position the copper seal between the CF flanges of the TM and of the plug-in by pre-tensioning the compensator. This concept was validated with the following tests: cycling pressure test (30,000 cycles), hydraulic (1000 hours, 6,5 m/s) and vibration tests followed by He leak tests in oven (room temperature and 4 MPa internal He pressure, 160°C and 2.8 MPa), mounting test. In the area of TM1V, the available space is so reduced that the lateral compensator was directly welded to the manifold (Fig. 7).

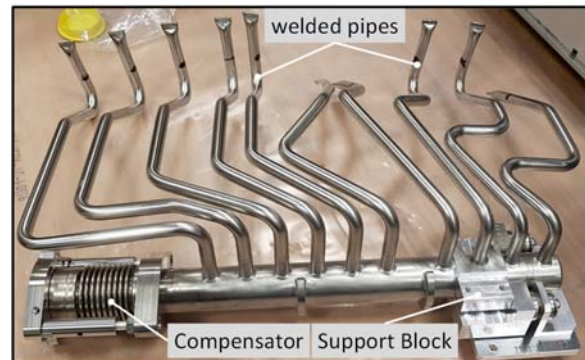


Fig. 7. Compensator welded to the manifold of TM1V. The pipes are already welded to the branches of the manifold before welding to the water connectors of the TEs.

The production of the 60 expansion joints was awarded to the company Witzenmann, Germany. Fabrication of the cages and mounting in the cages was made in ITZ. TIG orbital welding of the expansion joints to the manifolds of TM1V was made in ITZ.

Fig. 8 shows the finished water cooling system of TM1V. Due to the lack of space, the support structure were adapted to allow the pipe routing.

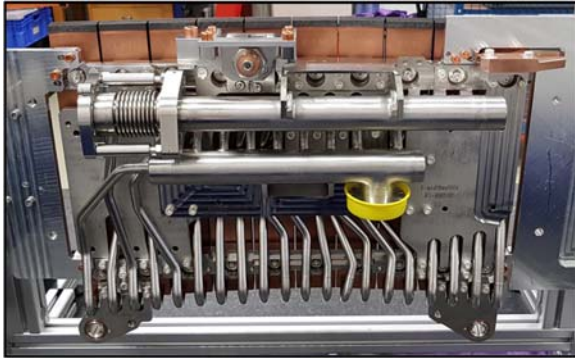


Fig. 8. View of the cooling system of a finished TM1V on its transport structure.

The TEs are water-cooled in parallel in the TMs. The dynamic pressure drop of the TEs was systematically measured with a $\pm 15\%$ tolerance with respect to the measured mean value. The dynamic pressure drop of the TMs was systematically measured and compared to the calculation performed with the FloMASTER software.

Table 2. Results of the dynamic pressure drop

TM type	ΔP_{min} (MPa)	ΔP_{max} (MPa)	Calc./ Meas.	Standard Deviation
TM1H	1,10	1,32	5%	0,63
TM2H	1,16	1,30	6%	0,40
TM3H	1,25	1,44	4%	0,58
TM4H	1,15	1,32	9%	0,67
TM1V	1,03	1,09	3%	0,16
TM2V	1,09	1,11	4%	0,09
TM3V	1,08	1,13	3%	0,14

The dynamic pressure drop was measured at room temperature for the working point defined for an axial velocity 10 m/s in the channel of the TEs, which is equipped with a twisted tape (twist ratio 2, 1mm thick, stainless steel). Table 2 shows a larger standard deviation for the TMs of the horizontal area, which reflects the deviation of the measurements of the individual TEs (length: 572-594 mm). The consequence was the decision to assign a position of the TMs in the divertor units to define the position of possible restrictions to balance the cooling loops outside the plasma vessel.

3.3 Results of the quality assessment of the target modules

The quality of the TMs was systematically assessed as follows: HHF loading in GLADIS, integral He leak and outgassing inspection, and visual inspection before packaging. The He leak rate and outgassing were

monitored in a vacuum oven: a leak rate $\leq 5 \cdot 10^{-7}$ Pa ℓ /s at room temperature and 4 MPa internal He pressure, and a leak rate $\leq 5 \cdot 10^{-6}$ Pa ℓ /s at 160°C and 2.5 MPa internal He pressure (1 cycle). During the cycle, the mass spectrometer measurement was compared to a reference spectrum, which indicated the acceptable levels for W7-X. All produced TMs successfully passed the integral leak test. At least one completed TM of each type (in total 14 TMs) was HHF loaded in the GLADIS facility to perform a thermal mapping of the 3D machined CFC surface. The spatially and temporally recorded thermal response to the well-defined heat flux could provide a reference for IR diagnostics during plasma operation of W7-X. Screening test with 15 s pulse length were performed at 6, 8, and 10 MW/m² as well as pulsed test at 10 MW/m² (2s on, 1s off, for 17,5s). After HHF testing, the visual inspection showed no damage, 3D measurement no change and deformation of the TM surface, and all tested TMs successfully passed the He leak rate inspection. These results confirmed that the produced TMs achieved the specified high performance for operation in W7-X.

4. Conclusion

The production of the last 70 TMs of the vertical and of the horizontal area) has been successfully finished. For the horizontal area, the main difficulty was to achieve the required tolerance of the divertor surface of the individual TMs due to the length of the TEs and integration of diagnostics in the divertor surface. For the vertical area, the main difficulty was the restricted space for the cooling system and in particular for the connection to the feeding pipes of the plug-ins. A special design of the water manifolds was needed but also lateral compensators were developed. The stepwise approach for the production of the TMs of the HHF divertor with a first set of 30 TMs (1/3) followed by the production of the remaining 70 TMs (2/3) allowed an efficient transfer of the gained experience and minimized the risk of using non reliable technical solutions. The quality assessment showed stable quality of the produced TMs. The HHF divertor production was completed and delivered to W7-X in 2019 on time; mounting operation of the target modules in the plasma vessel of W7-X has started and the plasma vessel is planned to be closed in 2021.

References

- [1] T. S. Pedersen, et al., First divertor physics studies in Wendelstein 7-X, Nucl. Fusion 59 (2019) 096014, doi: 10.1088/1741-4326/ab280f.
- [2] A. Peacock, et al., Progress in the design and development of a test divertor (TDU) for the start of W7-X operation, Fusion Eng. Des. 84 (2009) 1475-1478, doi : 10.1016/j.fusengdes.2009.01.053.
- [3] G. Ehrke, et al., Design and Manufacturing of the Wendelstein 7-X Cryo-Vacuum Pump, Fusion Eng. Des. 146 (2019) 2750-2760, doi : 10.1016/j.fusengdes.2009.05.020.
- [4] J. Boscary, et al., Design and technological solutions for the plasma facing components of Wendelstein 7-X, Fusion Eng. Des. 86 (2011) 572-575, doi : 10.1016/j.fusengdes.2010.11.020.

- [5] A. Peacock, et al., The procurement and testing of the stainless steel in-vessel panels of the Wendelstein 7-X Stellarator, *Fusion Eng. Des.* 86 (2011) 1706-1709, doi : 10.1016/j.fusengdes.2011.04.034.
- [6] B. Mendelevitch, et al., Lessons learned from the design and fabrication of the baffles and heat shields of Wendelstein 7-X, *Fusion Eng. and Des.* 88 (2013) 1660-1663, doi : 10.1016/j.fusengdes.2013.05.110.
- [7] H. Renner, et al., Physical aspects and design of the Wendelstein 7-X divertor, *Fusion Sci. Technol.* 46 (2004) 318-326.
- [8] A. Peacock, et al., Status of high heat flux components at W7-X, *IEEE Trans. Plasma Sci.* 42(3) (2014) 524-532, doi : 10.1009/TPS.2014.2302542.
- [9] J. Boscary, et al., Progress in the production of the W7-X divertor target modules, *Fusion Eng. and Des.* 146 (2019) 1975-1978, doi : 10.1016/j.fusengdes.2019.03.080.
- [10] J. Boscary, et al., Summary of the production of the divertor target elements of Wendelstein 7-X, *Fusion Eng. Des.* 124 (2017) 348-351, doi : 10.1016/j.fusengdes.2017.03.084.
- [11] H. Greuner, et al., Results and consequences of high heat flux testing as quality assessment of the Wendelstein 7-X divertor, *Fusion Eng. Des.* 88 (2013) 581-584, doi : 10.1016/j.fusengdes.2013.05.044.
- [12] P. Junghanns, et al., Repair process of Wendelstein 7-X target modules, *Fusion Eng. Des.* 146 (2019) 1166-1170, doi : 10.1016/j.fusengdes.2019.02.033.
- [13] P. Junghanns, et al., Local copper coating of the connectors of the divertor target elements of Wendelstein 7-X, *Fusion Eng. Des.* 124 (2017) 483-486, doi : 10.1016/j.fusengdes.2016.12.022.
- [14] P. Junghanns, et al., Experience gained with the 3D machining of the W7-X HHF divertor target elements, *Fusion Eng. Des.* 98-99 (2015) 1226-1230, doi : 10.1016/j.fusengdes.2014.11.018.
- [15] J. Boscary, et al., Design improvement of the target elements of the Wendelstein 7-X divertor, *Fusion Eng. Des.* 87 (2012) 1453-1456, doi : 10.1016/j.fusengdes.2012.03.034.